

High-pressure *Cmca* and *hcp* phases of germanium

K. Takemura,¹ U. Schwarz,² K. Syassen,^{3,*} M. Hanfland,⁴ N. E. Christensen,⁵ D. L. Novikov,⁶ and I. Loa³

¹National Institute for Research in Inorganic Materials, Namiki 1-1, Tsukuba, Ibaraki 305-0044, Japan

²Max-Planck-Institut für Chemische Physik fester Stoffe, Pirnaer Landstrasse 176, D-01257, Dresden, Germany

³Max-Planck-Institut für Festkörperforschung, Heisenbergstrasse 1, D-70569 Stuttgart, Germany

⁴European Synchrotron Radiation Facility, Boîte Postale 220, 38043 Grenoble, France

⁵Institute of Physics and Astronomy, Aarhus University, DK-8000 Aarhus C, Denmark

⁶Arthur D. Little Inc., Acorn Park, Cambridge, Massachusetts 02140-2390

(Received 23 June 2000)

Structural phase transitions of germanium at pressures up to 190 GPa have been investigated by means of angle-dispersive x-ray powder diffraction using synchrotron radiation. Near 100 GPa the primitive hexagonal modification of Ge transforms to an orthorhombic phase with 16 atoms per unit cell. The results of full-profile Rietveld refinements in space group *Cmca* indicate that the orthorhombic modification of Ge is isotypic to the phase Si-VI. Near 160–180 GPa Ge undergoes a transition to a structure assigned as hexagonal close packed (*hcp*). *Ab initio* calculations of pressure-dependent enthalpies and optimized structural parameters are presented for different structures of Ge. The calculated results clearly support the observed occurrence of the *Cmca* structure in Ge.

The structural properties of germanium at high pressures show some similarity to those of silicon (see Refs. 1–3 for related reviews). With increasing pressure Ge transforms from the diamond-type phase to the β -Sn-type structure near 10 GPa (Ref. 1) and to a hexagonal primitive (*hp*) phase with space group (SG) *P6/mmm* near 81 GPa.⁴ An intermediate orthorhombic phase (SG *Imma*) is observed at 75 to 80 GPa.⁵ Total energy calculations based on first-principle methods⁶ predict phase transitions in accordance with the structural sequence observed up to 90 GPa. At pressures higher than 100 GPa, Ge is reported⁴ to crystallize in a double-hexagonal close packed (*dhcp*) arrangement of atoms, corresponding to a mixed hexagonal (*hcp*) and cubic (*fcc*) stacking sequence of close packed layers. Recently, the crystal structure of the phase Si-VI which exists near 40 GPa, intermediate between *hp* and *hcp* (SG *P6₃/mmm*) modifications and originally assigned as *dhcp* (Ref. 3) was solved and refined on the basis of high-resolution x-ray powder diffraction data.⁷ Si-VI is found to adopt an unusual orthorhombic structure (space group *Cmca*, $Z=16$ atoms per cell), which is isotypic to the high-pressure modifications Cs-V (Ref. 8) and Rb-VI.⁹ Thus, experimental results suggest that Si and Ge, after passing through the *hp* structure, do not follow any more the same structural sequence at higher pressures.

Here we report results of angle-dispersive x-ray powder diffraction studies of Ge at pressures between 80 and 190 GPa. We find that a phase with a structure isotypic to that of Si-VI exists in a rather wide pressure range from about 100 to 160 GPa. Furthermore, near 180 GPa Ge transforms to a *hcp* modification. No indication was found for the existence of a *dhcp* phase of Ge around 100 GPa. The structural behavior of Ge at these very high pressures is of considerable interest for the theoretical modeling of the phase stability of group-IV elements at extreme conditions. Thus, we have also explored theoretically the stability of the new phases of Ge relative to other test structures using density functional theory.

Diffraction experiments were carried out at the undulator beamline ID9 of the European Synchrotron Radiation Facility Grenoble. Pressures were generated using a diamond anvil cell. The results presented below were obtained in two experimental runs up to 135 and 190 GPa, performed with bevelled anvils of flat-culet diameters of 150 and 50 μm , respectively. Re gaskets with initial hole diameters of 40–50 μm were used. High-purity Ge was ground into a fine powder and placed in the gasket using a 4:1 methanol/ethanol mixture as a pressure transmitting medium. Diffraction patterns were recorded on an image plate. X-ray wavelength ($\lambda=0.45222$ Å) and detector-to-sample distance (~ 0.3 m) were calibrated using a standard Si reference sample. Integration of the two-dimensional diffraction patterns was performed using the Fit2D software.¹⁰ Pressures were partly determined by the ruby luminescence method.¹¹ The ruby signal was lost in measurements above 100 GPa. In these cases the x-ray beam (15 μm diam) was focused on the inner rim of the gasket hole and Bragg reflections of Re were used to determine the pressure based on the pressure-volume (PV) relation given in Ref. 12. The estimated uncertainty in pressure is of the order $\pm 5\%$.

Selected diffraction diagrams of Ge are shown in Fig. 1. At pressures up to 93 GPa, our results are in accordance with a pure *hp* phase [$a=2.4631(4)$ Å, $c=2.2917(6)$ Å, $c/a=0.930$ at 83 GPa]. At 99 GPa, the appearance of additional diffraction lines indicates the onset of a structural transition to a new phase. At 114 GPa, all diffraction lines of *hp*-Ge have disappeared and we observe only lines of the new phase and possibly a small admixture of a *hcp* phase (see below). Further increase of pressure up to 160 GPa induces only minor changes of the diffraction diagrams but diffraction peaks broaden. Pronounced changes in the diffraction patterns near 180 GPa indicate another structural phase transition. All intense reflections of diffraction diagrams taken at 180 and 190 GPa can be indexed on the basis of a *hcp* phase [180 GPa: $a=2.398(3)$ Å, $c=3.909(5)$ Å, $c/a=1.630$ at

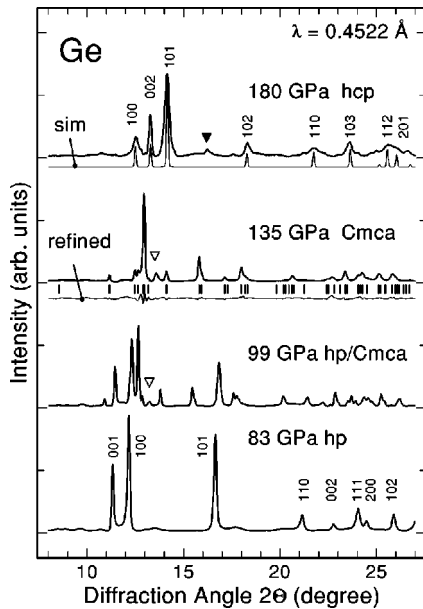


FIG. 1. High-pressure x-ray diffraction patterns of Ge. The sequence of stable modifications for increasing pressures is hexagonal primitive (hp) at 83 GPa, *Cmca* (Cs-V type) coexisting with hp-Ge at 99 GPa, *Cmca* at 135 GPa, and hcp at 180 GPa. The open and closed triangles point to reflections which are attributed to small admixtures of the hcp and *Cmca* phases, respectively. The curve marked “refined” is the difference between experimental diffraction diagram at 135 GPa and refined *Cmca* model. The curve marked “sim” represents a simulated diffraction diagram for the hcp structure.

180 GPa]. A simulated hcp profile is shown below the 180 GPa pattern in Fig. 1. Assuming a dhcp instead of a hcp arrangement does not account for additional weak reflections seen in the experimental diagram at 180 GPa. However, some admixture of the lower pressure *Cmca* phase is still present, as, for instance, indicated by the large intensity of the 002 reflection and several additional peaks at positions expected for the intermediate phase. The observations on the emergence of new phases in Ge are qualitatively similar to those for Si: the intermediate phase Si-VI was found to coexist with either the lower pressure hp phase or the higher pressure hcp phase.

The diagrams of Ge measured between 114 and 160 GPa cannot be indexed on the basis of a dhcp lattice. On the other hand, a strong similarity to the diffraction patterns of Si-VI is obvious. Thus, we have performed full profile Rietveld refinements using the *Cmca* structure model of Si-VI. For the 135 GPa diagram in Fig. 1 we show the difference between the experimental data and the refined profile. One peak, marked by open triangles in Fig. 1, was excluded from the refinements. It appears to be due to a small admixture of the higher pressure hcp phase. The refinement was performed using GSAS.¹³ Texture effects were taken into account by a spherical harmonics model.¹⁴ The obtained $R(F^2)$ value (residual for intensities) amounts to 9.6%. Despite the rather extreme pressure conditions, the fit is only slightly poorer than in the case of the analogous Si-VI data (7.6%). The results of the refinement clearly suggest the *Cmca* structure with $Z=16$ to be the correct model for the high-pressure modification of Ge.

TABLE I. Observed and calculated structural parameters of Ge at 135 GPa (space group *Cmca*, $Z=16$). Data for the isotopic high-pressure phase Si-VI (Ref. 7) are listed for comparison. The coordinates for 8*d* and 8*f* sites are $(x,0,0)$ and $(0,y,z)$, respectively. The distance labeled d_1 is the shortest (8*f*–8*f*) atom contact; V_0 refers to the ambient pressure volume (22.64 \AA^3) at 298 K.

	Ge expt.	Ge calc.	Si-VI expt.
P(GPa)	135	135	42.5
$a(\text{\AA})$	7.885(2)	7.886	7.9686
$b(\text{\AA})$	4.655(1)	4.656	4.7759
$c(\text{\AA})$	4.651(1)	4.667	4.7546
$x(8d)$	0.218(1)	0.2210	0.219
$y(8f)$	0.164(2)	0.1721	0.172
$z(8f)$	0.313(1)	0.3138	0.328
$R(F^2)$	0.096	-	0.075
$V_{\text{atom}}(\text{\AA}^3)$	10.67(6)	10.71	11.308
V/V_0	0.4713	0.473	0.565
a/c	1.695	1.6899	1.676
b/c	1.001	0.9978	1.004
$d_1(\text{\AA})$	2.315	2.369	2.321

The orthorhombic unit cell parameters at 135 GPa are given in Table I. The deviation from a tetragonal metric is extremely small. The *Cmca* crystal structure is characterized by two crystallographically different types of atoms on Wyckoff sites 8*d* and 8*f*, respectively. The corresponding positional parameters (see Table I) are very close to those reported for the phase Si-VI, i.e., the two phases are isotopic. The *Cmca* structure was previously interpreted in terms of a distorted fcc structure.⁸ An alternative interpretation as a pseudohexagonal structure becomes obvious when considering an eight-atom primitive monoclinic cell in a suitable setting (SG 14, $P12_1/n1$), as shown in Fig. 2. The relations between orthorhombic and monoclinic lattice parameters are $a_m = c_m = \sqrt{a_o^2 + c_o^2}/2$ (4.5783 \AA at 135 GPa) and $b_m = b_o$. The monoclinic angle ($\beta = 61.1^\circ$) is close to 60° . Therefore, the *Cmca* structure can be viewed as a slightly distorted

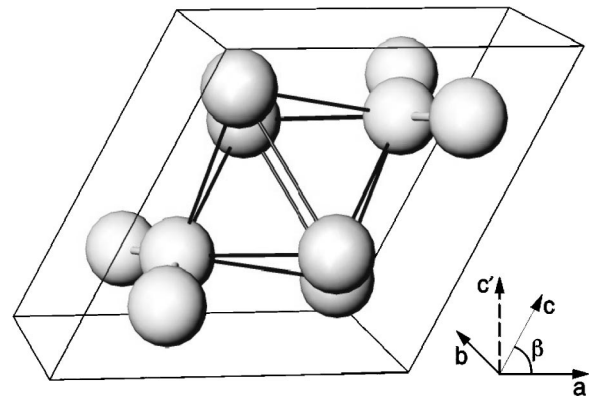


FIG. 2. Schematic representation of the orthorhombic (*Cmca*, $Z=16$) structure of Ge using a monoclinic primitive unit cell ($Z=8$). The monoclinic cell is pseudohexagonal ($a_m = c_m$, $\beta = 61.1^\circ$). The axes shown in the figure refer to the monoclinic cell. The c' direction is perpendicular to the ab plane. Dark lines between atoms indicate an octahedral interstitial site.

hexagonal Bravais lattice with eight atoms per cell. The actual orientation relation between *Cmca* and hcp phases, however, could be different. Similar observed d spacings suggest that buckled (202) planes of *Cmca* (horizontal in Fig. 2) could become (001) planes in hcp. Such a relation would be compatible with the orientation of octahedra around interstitial sites in *Cmca* (see Fig. 2) and hcp. We also note that a slight change in the monoclinic angle towards 58.52° would result in a four-layer repeat unit along c' (Fig. 2).

Our experimental results do not confirm the earlier report of a dhcp high-pressure modification of Ge appearing near 100 GPa.⁴ The authors showed no experimental data we could compare with here. The volume they give at 125 GPa is $\sim 5\%$ smaller than that for Ge *Cmca* at this pressure. Very likely, the energy-dispersive diffraction method used in the earlier study did not offer the resolution and sensitivity necessary to detect small deviations from a hexagonal metric and weak reflections characteristic of the *Cmca* structure.

We have examined theoretically the stability of Ge using the local density approximation (LDA) to the density-functional theory. The semicore $3d$ states were treated as relaxed band states on the same footing as the $4s$ and $4p$ valence states. The $3s$ and $3p$ were relaxed also, but they were calculated in a separate, lower energy panel. In the presence of occupied d states at energies not too far below the Fermi level, straight LDA calculations lead to a significant overbinding.^{15,16} In Ge this effect is in particular affecting the PV relation for compressed lattices. As in earlier calculations for Sn ($4d$ states) (Ref. 15) and Zn ($3d$) (Ref. 16) we compensate for this LDA error by applying a downshift in each iteration towards self-consistency of the d states. A shift of 2 eV was used, as in the case of Zn. One may consider this an ‘‘LDA+ U treatment’’¹⁷ of the filled $3d$ bands. Atomic coordinates as well as cell dimensions are optimized simultaneously at constant volume by minimizing the total energy via a steepest descent method. The solution of the effective one-electron equations was performed by means of the linear muffin tin orbital method¹⁸ in the full-potential version.^{19,20} Having calculated the optimized total energy E vs volume V for a given modification, we derive the PV relation which is then used to calculate the enthalpy $H(P) = E + PV$.

Portions of the calculated PV relations for the hp, *Cmca*, and hcp phases are shown in Fig. 3, together with the experimental PV data. Taking into account experimental errors in the pressure determination, the agreement between calculated and experimental data is very good. Near 100 GPa the calculated volume difference between hp and *Cmca* is about -1.7% , while that between *Cmca* and hcp is only -0.7% at 180 GPa. The optimized c/a axial ratios for hp and hcp, respectively, are 0.93 and 1.62 with essentially no change with volume. These ratios are in close agreement with the experimental results. For dhcp we find $c/a = 3.625$, about two times the hcp value and also volume independent. The optimized parameters for the *Cmca* structure at 135 GPa are listed in Table I. Axial ratios as well as positional parameters converge towards the experimental values, as is also the case for optimized parameters of the *Cmca* phases Si-VI (Ref. 21) and Cs-V.²²

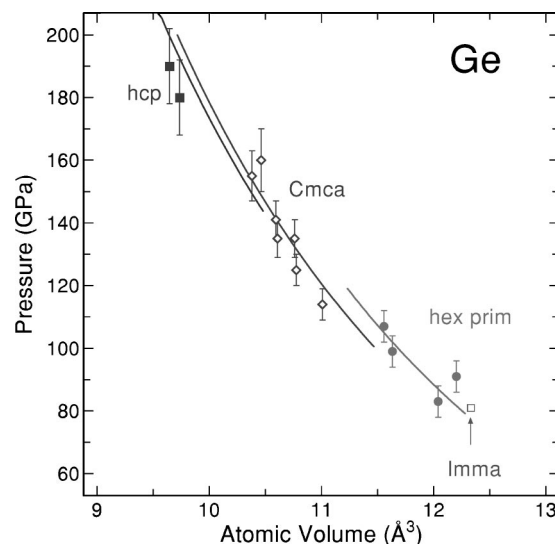


FIG. 3. Pressure as a function of atomic volume for the hp, *Cmca*, and hcp phases of Ge. Symbols and lines represent experimental data and calculated PV relations, respectively. The single data point for the *Imma* phase is from Ref. 5.

Figure 4 shows the calculated enthalpies vs pressure for six modifications of Ge considered here. Allowing for ± 0.5 mRy numerical error in the total energies, the calculations suggest that the *Cmca* structure has the lowest enthalpy between 80 ± 5 GPa and 170 ± 20 GPa. The calculated transition pressure for the $hp \rightarrow Cmca$ transition is close to the experimental result. The hcp structure clearly is lowest in enthalpy above ~ 280 GPa all the way up to at least 1 TPa. The fcc and dhcp structures are found to have significantly higher enthalpies compared to *Cmca* and hcp. The calculations indicate that a bcc phase may occur intermediate between the *Cmca* and hcp phases, which is not observed experimentally. We note that the calculated results for the stability of bcc and hcp phases relative to *Cmca* depend critically on details of the band structure calculations. For instance, if the $3d$ states are not downshifted, then up to 600 GPa bcc would always be higher in enthalpy with respect to *Cmca* by 5–10 mRy/atom, and the transition *Cmca* \rightarrow hcp would be shifted up to 500 GPa, even if the generalized gradient approach (GGA) (Ref. 23) is used. Presumably, the

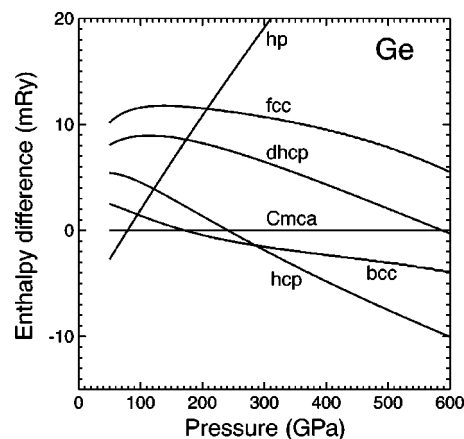


FIG. 4. Calculated enthalpy differences for different structures of Ge relative to the optimized *Cmca* structure.

GGA could be adjusted^{24,25} by “tuning” the coefficient κ in the enhancement factor F_X (see Ref. 23) which is directly associated with the degree of localization of the exchange-correlation hole.

In summary, angle-dispersive x-ray diffraction studies of Ge up to 190 GPa show that an orthorhombic phase exists intermediate between the hp phase and the newly detected hcp phase, i.e., at pressures between about 100 and 170 GPa. Full profile refinements of diffraction diagrams of the orthorhombic phase in space group *Cmca* ($Z=16$) yield axial ratios and atom position parameters very similar to those of Si-VI stable near 42 GPa. The *Cmca* structure can be inter-

preted as a slightly distorted hexagonal Bravais lattice with eight atoms per unit cell. In agreement with experiment, our total energy calculations suggest that the *Cmca* phase is lowest in energy at pressures between about 80 and 170 GPa. The calculations also indicate that hcp is more stable than the *Cmca* phase at pressures above 280 GPa. Predictions for the phase stable above 170 GPa depend on details of the band structure calculations.

Note added. After submission of this manuscript we became aware of a preprint by J. F. Ribeiro and M. L. Cohen. They report *ab initio* pseudopotential calculations of the phase stability of Ge at very high pressures.

*Corresponding author. Email address: k@syassen.de

¹C. S. Menoni, J. Z. Hu, and I. L. Spain, *Phys. Rev. B* **34**, 362 (1986).

²A. L. Ruoff and T. Li, *Annu. Rev. Mater. Sci.* **25**, 249 (1995).

³R. J. Nelmes, M. I. McMahon, in *High Pressure in Semiconductor Physics* (Academic, New York, 1998), Vol. 1, p. 146.

⁴Y. K. Vohra, K. E. Brister, S. Desgreniers, A. L. Ruoff, K. J. Chang, and M. L. Cohen, *Phys. Rev. Lett.* **56**, 1944 (1986).

⁵R. J. Nelmes, H. Liu, S. A. Belmonte, J. S. Loveday, M. I. McMahon, D. R. Allan, D. Häussermann, and M. Hanfland, *Phys. Rev. B* **53**, R2907 (1996).

⁶S. P. Lewis and M. L. Cohen, *Solid State Commun.* **89**, 483 (1994).

⁷M. Hanfland, U. Schwarz, K. Syassen, and K. Takemura, *Phys. Rev. Lett.* **82**, 1197 (1999).

⁸U. Schwarz, K. Takemura, M. Hanfland, and K. Syassen, *Phys. Rev. Lett.* **81**, 2711 (1998).

⁹U. Schwarz, K. Syassen, A. Grzechnik, and M. Hanfland, *Solid State Commun.* **112**, 319 (1999).

¹⁰A. P. Hammersley, S. O. Svensson, M. Hanfland, A. N. Fitch, and D. Häussermann, *High Press. Res.* **14**, 235 (1996).

¹¹H. K. Mao, P. M. Bell, J. W. Shaner, and D. J. Steinberg, *J. Appl. Phys.* **49**, 3276 (1978).

¹²Y. K. Vohra, S. J. Duclos, and A. L. Ruoff, *Phys. Rev. B* **36**, 9790 (1987). The isothermal equation of state of Re given in this reference is based on the reduced shock wave data of R. G. McQueen *et al.*, in *High Velocity Impact Phenomena*, edited by

R. Kinslow (Academic, New York, 1970), p. 293.

¹³A. C. Allen and R. B. Von Dreele, Los Alamos Natl. Laboratory Report No. LAUR 86-748 (1994) (unpublished).

¹⁴See L. B. McCusker, R. B. Von Dreele, D. E. Cox, D. Louer, and P. Scardi, *J. Appl. Crystallogr.* **32**, 36 (1999), and references therein.

¹⁵N. E. Christensen and M. Methfessel, *Phys. Rev. B* **48**, 5797 (1993).

¹⁶D. L. Novikov, A. J. Freeman, N. E. Christensen, A. Svane, and C. O. Rodriguez, *Phys. Rev. B* **56**, 7206 (1997).

¹⁷A. I. Liechtenstein, V. I. Anisimov, and J. Zaanen, *Phys. Rev. B* **52**, R5467 (1995).

¹⁸O. K. Andersen, *Phys. Rev. B* **12**, 3060 (1975).

¹⁹M. Methfessel, *Phys. Rev. B* **38**, 1537 (1988).

²⁰M. Methfessel and M. van Schilfhaarde (unpublished); (private communication).

²¹N. E. Christensen, D. L. Novikov, and M. Methfessel, *Solid State Commun.* **110**, 615 (1999); R. Ahuja, O. Eriksson, and B. Johansson, *Phys. Rev. B* **60**, 14 475 (1999).

²²K. Takemura, N. E. Christensen, D. L. Novikov, K. Syassen, U. Schwarz, and M. Hanfland, *Phys. Rev. B* **61**, 14 399 (2000).

²³J. P. Perdew, K. Burke, and M. Ernzerhof, *Phys. Rev. Lett.* **77**, 3865 (1996).

²⁴E. L. Peltzer y Blancá, C. O. Rodriguez, J. Shitu, and D. L. Novikov (unpublished).

²⁵S. Tinte, M. G. Stachiotti, C. O. Rodriguez, D. L. Novikov, and N. E. Christensen, *Phys. Rev. B* **58**, 11 959 (1998).